



1 **A Low-cost UAV Coordinated Carbon Observation**
2 **Network (LUCCN): an analysis of environment impact**
3 **on ground base measurement node**

4 Xiaoyu Ren^{a,b}, Dongxu Yang^{a,b*}, Yi Liu^{a,b}, Yong Wang^c, Ting Wang^{a,b}, Zhaonan Cai^{a,b},
5 Lu Yao^{a,b}, Tonghui Zhao^{a,b}, Jing Wang^{a,b}, Zhe Jiang^{a,b}

6 ^aCarbon Neutrality Research Center (CNRC), Institute of Atmospheric Physics, Chinese Academy of
7 Sciences, Beijing 100029, China

8 ^bKey Laboratory of Middle Atmospheric Physics and Global Environment Observation (LAGEO),
9 Institute of Atmospheric Physics, Chinese Academy of Sciences, Beijing 100029, China

10 ^cNanjing Ztweather Technology CO., LTD, Nanjing 210044, China

11 *Correspondence to* : Dongxu Yang (yangdx@mail.iap.ac.cn)

12 **Abstract.** Most anthropogenic carbon dioxide (CO₂) emissions originate from urban areas. To improve
13 understandings of urban and regional emissions, we design and construct a low-cost UAV coordinated
14 carbon observation network (LUCCN) which uses mid-accuracy (± 1 ppm) CO₂ sensors. In this paper,
15 we introduce our multi-variable non-linear regression method for calibrating the non-dispersive
16 infrared (NDIR) CO₂ sensors for LUCCN's ground stations. We tested our calibration method with
17 concentration data collected at the Xinglong Atmospheric Background Observatory. With comparison
18 against data simultaneously collected by a high-accuracy cavity ring-down spectrometer, we found the
19 maximum standard deviation of LUCCN's sensors to be 0.782 ppm in a controlled laboratory
20 environment with a 1-second window size and 0.53 ppm in an outdoor environment with a 1-hour
21 running average window size. As validation of LUCCN's ground measurements, we identify and
22 present consistent trends between local CO₂ concentration variations and aerosol pollution events
23 captured by the space-based moderate resolution imaging spectrometer (MODIS).

24 **Keywords:** CO₂ concentration, Regional emissions, Low-cost network (LUCCN), Ground base
25 measurement

26 **1 Introduction**

27 Anthropogenic emission of Carbon Dioxide (CO₂) is a primary driver of climate change and
28 global warming (Rosenzweig et al., 2010). Investigations on anthropogenic emission from fossil fuel
29 combustion require a complete measurement system to the important sectors, e.g. energy, industry and
30 city (Liu et al., 2014). The inventory method (bottom-up method) is the foundation to understand the
31 condition of anthropogenic emission of each country and sector. Unfortunately, the dis-transparency
32 and bias of inventory is a long live hot-topic to be discussed, even a standard inventory metrology has
33 been reserved in 2006 IPCC Guidelines for National Greenhouse Gas Inventories, and refined for



34 several versions (Andres et al., 2014; Bréon et al., 2015; Broquet et al., 2016). Therefore, the
35 independent method and atmospheric inversion have been included in 2019 refinement to verify
36 emission inventories (Maksyutov et al., 2019). State-of-art atmospheric inversion methods provide near
37 real-time optimization of an acknowledged inventory. The improvement of inversion depended on the
38 method and also measurement. Lack of measurement cannot effectively optimize the existing inventory
39 (Duren et al., 2012). Unlike natural carbon emission processes e.g. ecosystem and ocean,
40 anthropogenic emission sources are more concentrated with frequently varying emission rates (Kim et
41 al., 2018). Therefore, monitoring anthropogenic emissions with atmospheric inversion methods
42 requires dense and continuous measurements of CO₂ concentration variations with high quality
43 (Broquet et al., 2016; Arzoumanian et al., 2019).

44 Ground-based CO₂ measurements gained significant progress in the last decade (Kort et al., 2013;
45 Turnbull et al., 2015; Delaria et al., 2021). Systematic ground-based observations of CO₂ began in
46 Hawaii in the 1950s, and international ground-based observation networks, such as the European
47 Integrated Carbon Observation System (ICOS) (<https://www.icos-ri.eu/>, last access: 21 October 2023),
48 the International Atmospheric Greenhouse Gas Monitoring Network (GAW) (Ries, 2013) and other
49 greenhouse gas observation systems (Staufner et al., 2016; Delaria et al., 2021), have been gradually
50 established to carry out continuous observations of ground-based greenhouse gases. For example, the
51 GAW ground-based observation network has 31 global atmospheric background stations and more than
52 400 stations for regional GHG observations. Those international ground-based observation networks
53 have conducted long-term, high-precision observations of ground-based greenhouse gases and are the
54 main data sources for international scholars to monitor and assess global greenhouse gas emissions
55 (Agusti-Panareda et al., 2022; Bao et al., 2022).

56 International ground-based observation networks play an important role in regional and
57 continental scale greenhouse gas detection and assessment. Although observation networks like ICOS
58 and GAW cover large areas, their measurements can hardly describe emissions in smaller regions, e.g.
59 city and industry (Park et al., 2020). Therefore, we need denser networks to improve the spatial
60 coverage and resolution on CO₂ emissions, while the new network can also contribute to the larger
61 regional scale ground-based observation networks (Turner et al., 2016; Wu et al., 2016).

62 Many cities have carried out denser continuous ground-based measurements of CO₂ and other
63 greenhouse gases. For instance, the Megacity Carbon Project and the MegaParis CO₂ Project use



64 high-precision in-situ measurements from cavity ring-down spectrometers (Picarro G2301 and G2401)
65 to establish ground-based observation networks in Los Angeles and Paris (Irène et al., 2017; Verhulst
66 et al., 2017). For both projects, the hourly measurement accuracy of CO₂ emissions observations in
67 Paris and Los Angeles is 1 ppm, with the monthly average uncertainty of 10%. (Staufer et al., 2016;
68 Verhulst et al., 2017). Although high-precision spectrometers can provide high-quality observations
69 and analysis, they are expensive to manufacture and maintain (Park et al., 2020). Therefore, only a few
70 megacities, such as Los Angeles and Paris, have established observation stations or networks, while
71 most municipalities cannot afford the same. Nevertheless, to minimise measurement errors of urban
72 CO₂ fluxes, we need to maximise the density of ground stations.

73 To overcome the above limitations and to extend the observation coverages of CO₂ emissions,
74 low-cost CO₂ ground observation sensors have been used in urban-intensive CO₂ ground observations
75 (Liu et al., 2021). Although sensors of lower cost are usually less accurate, Broquet et al. (2016)
76 showed that the number of instruments is more important than the accuracy of their individual sensors,
77 and when sensors are densely deployed, the observation error could be significantly reduced (Turner et
78 al., 2016). In short, low-cost and denser networked detection of CO₂ is more desirable.

79 Currently, several low-cost CO₂ ground observation networks have been established for
80 continuous observations. For example, the Berkeley Atmospheric CO₂ Observation Network
81 (BEACO₂N) has used a large number of low-cost sensors (about fifty sensors) to establish a CO₂
82 detection network in San Francisco, and the distance between the adjacent instruments are
83 approximately 2 km (Broquet et al., 2016; Shusterman et al., 2018; Teige et al., 2016). In addition, Lee
84 et al. (2017) developed a mobile CO₂ observation network in Vancouver with low-cost sensors. The
85 network captures a CO₂ concentration map at street level that can verify city-level emission inventories.
86 Other previous studies presented that low-cost and denser CO₂ observation networks can help to study
87 the characteristics of urban CO₂ concentrations. In summary, lower cost ground observation network
88 can measure concentration distribution with medium accuracy (± 1 ppm) while having greater
89 coverages (Broquet et al., 2016; Turner et al., 2016; Arzoumanian et al., 2019).

90 In this article, we introduce the ground station for our novel low-cost UAV coordinated carbon
91 observation network (LUCCN), which uses non-dispersive infrared (NDIR) CO₂ sensors. Comparing to
92 networks using high-accuracy sensors, LUCCN's ground station is cheaper to manufacture and
93 maintain, easier to operate and move around. Such characteristics are crucial to enable denser



94 networked detections of CO₂. The rest of this article consists of four sections. Section 2 introduces the
95 LUCCN sensors, including the principle of instrument observation and the components of the
96 instrument. Section 2 also presents the laboratory calibration methods, results and instrument
97 performances of LUCCN nodes. In order to further verify the observation performance of LUCCN, we
98 present the outdoor continuous observation data calibration results in Section 3. We also compared
99 outdoor observations against data simultaneously collected by a high-accuracy spectrometer. Finally,
100 we prove LUCCN's effectiveness by showing consistent pollution-caused trends from satellite
101 observations and LUCCN's measurements.

102 **2 Ground-based node of A Low-cost UAV Coordinated Carbon observation Network (LUCCN)**

103 **2.1 Instrument**

104 The main component of LUCCN includes a swam of ground-based nodes. In each sensor site, a
105 series of commercial sensors are organized in a small sized newly designed weatherproof enclosure.
106 We use a Vaisala CarboCap GMP343 for CO₂ measurement in Figure 1(b). This sensor has been
107 introduced and well tested in Berkeley Atmospheric CO₂ Observation Network (BEACO₂N) studies
108 (Delaria et al., 2021; Kim et al., 2018; Shusterman et al., 2018), which presented excellent stability in
109 long term data collections of CO₂ concentrations.

110 In this study, we test the accuracy performance of GMP343 in varied measurement environment,
111 incl. temperature, pressure and humidity. Variations of the three parameters fundamentally impact the
112 measurement accuracy by altering infra-red light source intensity and gas molecule absorptions.
113 Additionally, environmental impacts to accuracies vary between individual sensors due to
114 manufacturing precisions and factory calibration methods. Beyond the CO₂ sensor, each network node
115 contains a slot to install sensors measuring co-emitted pollutant (CO, NO₂, PM_{2.5}), which help us to
116 determine source emission sectors. For example, we use AlphaSense CO and NO₂ electrochemistry
117 sensors which are common used in GHG observation networks. However, the response time of those
118 sensors are longer than the CO₂ NDIR sensors. The coordinate measurement is in-sufficient in a minute
119 temporal scale. The life-age of a electrochemistry is limited as 1 year. Considering the economical
120 efficiency and stable, the standard of LUCCN node we recommended is only contain CO₂ sensor as
121 atmosphere composition sensor, but the measurement function in a site.



122 **Fig. 1.** The internal structure of Luccn and the observation field diagrams in the laboratory. (a) is the exterior
123 diagram of Luccn ground stations, and (b) shows the internal composition of Luccn. (c) shows the NDIR
124 sensors and gas conduits placed inside a cloud chamber where temperature, pressure and humidity can be adjusted
125 according to demands. (d) shows the exterior of cloud chamber, Picarro G2301 and WMO CO₂ standard gas
126 cylinders.

127 In order to correct the bias induced by measurement environment, we integrate the pressure and
128 humidity sensors within individual nodes. Since there are pt1000 temperature sensors within all
129 GMP343's chambers, external temperature sensors are unnecessary. For flux inversions, we integrate a
130 Vaisala WXT-536 supersonic anemometer for measuring wind speed and directions. Finally, sensors
131 for each node are integrated within a custom designed weatherproof enclosure. We also optimized the



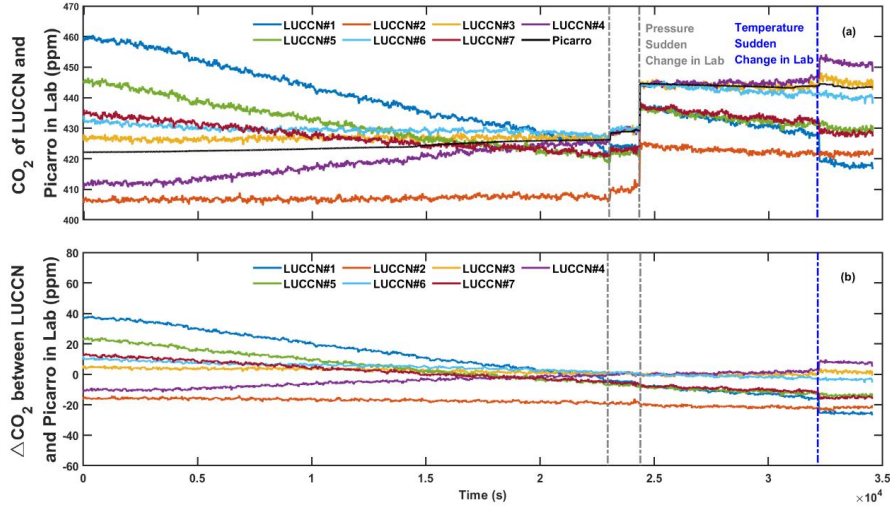
132 closure design for alternative mounting requirements.

133 To facilitate network data transmission and storage, we developed dedicated Internet of Things
134 infrastructure and database. For data security considerations, the database software can be used for
135 each local network without centralised storage. The total power supply requirement is less than 5 W
136 which allows us to use solar panels instead of electric cables in extreme environments.

137 **2.2 Performance and calibration in lab**

138 The previous chamber tests indicate significant biases resulting from environmental parameters,
139 including pressure, temperature, and humidity (Teige et al., 2016; Arzoumanian et al., 2019; Müller et
140 al., 2020; Delaria et al., 2021). As a solution, we have developed a bias-correction method to reduce the
141 environment-induced biases based on the standard manufacturer corrections. In our calibration process,
142 each sensor has to be calibrated in an environment-controlled chamber that could adjust the
143 temperature, pressure and humidity accurately (Figure 1c). The environment-controlled chamber used
144 in this study is provided by Beijing Municipal Meteorological Bureau. There were seven LUCCN
145 ground-based nodes and a Picarro G2301 involved in the calibration test at the same time. As
146 measurement references, we connected a Picarro G2301 spectrometer to the environment-controlled
147 chamber via an airtight tube. The Picarro G2301 was calibrated every 2 hours by WMO standard gas
148 (402 ppm CO₂) as shown in Figure 1d to remove the drift.

149 Figure 2(a) shows the CO₂ dry mole fractions measured by LUCCN nodes (colored lines) and the
150 Picarro sensor (black line). Evidently, there are notable differences between the measurements of
151 LUCCN nodes and the Picarro sensor in Figure 2(b). In addition, LUCCN sensors' performances vary
152 especially when there are pressure (gray dashed lines) and temperature mutations (blue dashed line) in
153 the chamber. In the case of sudden temperature change, LUCCN # 2, LUCCN # 5, and LUCCN # 6
154 experience negligible variations, while values of both LUCCN # 3 and 4 noticeably increase. On the
155 contrary, when the temperature suddenly changes, the values of LUCCN # 1 decrease significantly,
156 while LUCCN # 7 decrease slightly. Similarly, when the pressure changes suddenly, the measurement
157 deviations of LUCCN sensors are also slightly different. The differences in these numerical mutations
158 are also shown in Figure 2(b). The above phenomena indicate that even in the same environment,
159 different LUCCN sensors respond differently to environmental mutations. So it is necessary to
160 calibrate each LUCCN sensor respectively.



161 **Fig. 2.** (a) CO₂ mole fractions measured by seven LUCCN nodes in the lab (colored lines), as well as the
 162 synchronous measurement by the Picarro sensor (black line). (b) The differences (ΔCO_2) between the
 163 measurement of LUCCN nodes and Picarro G2301 corresponding to the top image. The vertical gray dotted lines
 164 in the two figures represent the moment of sudden changes in pressure inside the cloud chamber, while the vertical
 165 blue dotted lines represent the moment of the sudden change in temperature. Among them, different LUCCN
 166 nodes exhibit the inconsistent performance during sudden environmental changes, so they need to be calibrated
 167 separately.

168 We employ a multi-variable non-linear regression function to establish the relation between
 169 environment parameters and the measurement bias of CO₂ concentration. In our test, we found the bias
 170 correlation changes with pressure, temperature, humidity, and CO₂ concentration itself, hence we need
 171 to calibrate sensor measurements within all possible conditions through a multi-variable function.
 172 Furthermore, we also found the correlation between biases of CO₂ concentration, and environment
 173 parameters are non-linear. Finally, the bias correction changes with sensors. Thus, we need to correct
 174 biases of individual sensors respectively.

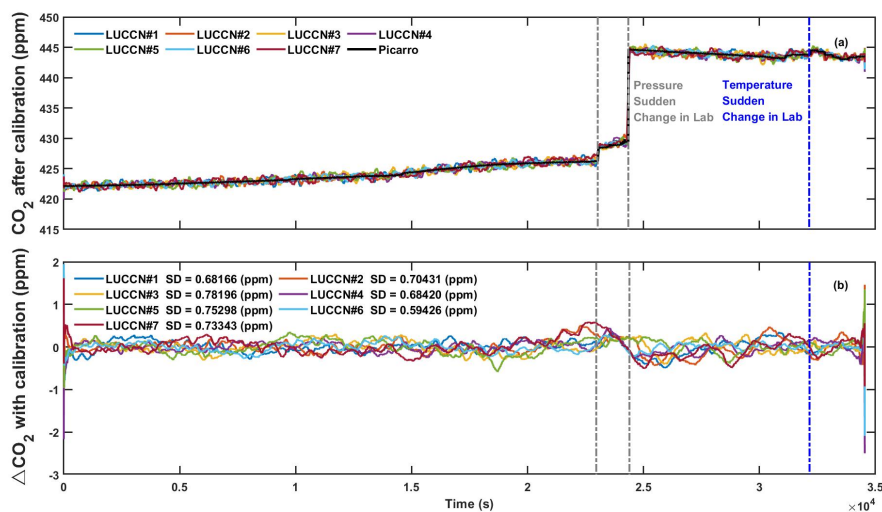
175 The multi-variable non-linear regression function to correct the bias shows,

$$176 \Delta CO_{2,calibration} = \sum_n^i a_i * T^i + \sum_n^i b_i * P^i + \sum_n^i c_i * W^i + \sum_n^i d_i * C^i + e \quad (1)$$

177 In which $\Delta CO_{2,calibration}$ represents the bias ($CO_{2,LUCCN} - CO_{2,G2301}$). T , P , W and C correspond to
 178 the internal temperature, the air pressure, the water vapor pressure and CO₂ concentration. In addition,
 179 a , b , c and d are the correction coefficients of T , P , W and C respectively. e is the baseline
 180 offset.



181 We applied the above correction method to a section of test data before deriving the coefficients
182 shown in eq.(1) for calibrating the entire test dataset. Figure 3(a) shows the calibration results of
183 LUCCN (coloured lines), and Figure 3(b) shows the differences between LUCCN and reference G2301.
184 Overall, the corrections are sufficient to offset the biases. Compared with Figure 2(b), the differences
185 have been reduced obviously, and the remained biases are very low. The standard deviations (SD) of
186 $\Delta\text{CO}_{2,\text{calibration}}$ of LUCCN sensors are all less than 1 ppm, and the maximum and minimum of SD are
187 0.782 ppm and 0.594 ppm respectively. We also test the orders of magnitude used in this regression
188 and find that the non-linear effect is not significant, which means lower orders, e.g. 3 order is enough
189 even when the parameters, such as pressure and temperature, changes dramatically. It may be due to
190 the data have been measured in the cloud chamber, so the calibration results perform better. The
191 calibration results might be overly optimistic due to stable environmental conditions provided by the
192 chamber, which isolate external environmental variations. Therefore, based on long-term and
193 continuous ground observations, the accuracy, sensitivity and drift of LUCCN would be further
194 verified in Section 3 and Section 4.



195 **Fig. 3.** (a) CO₂ mole fractions of LUCCN nodes with calibration (coloured lines) compared to the Picarro G2301
196 (black line); (b) The differences between the calibrated LUCCN nodes and Picarro G2301 corresponding to Figure
197 2(b). Compared with Figure 2(b), it can be seen that the effects of temperature and pressure fluctuations on the
198 response of LUCCN have been eliminated through the calibration. The standard deviations (SD) of LUCCN
199 nodes with calibration are all less than 1 ppm. The gray dotted lines and blue dotted lines in the figures represent
200 the same content as Fig. 2.



201 **3 Measurement**

202 **3.1 Observation site and setup**

203 LUCCN ground base nodes have been placed at the Xinglong Atmospheric Background
204 Observatory (Xinglong site) of the Institute of Atmospheric Physics of the Chinese Academy of
205 Sciences. Xinglong site is located on the top of Lianzhai Mountain (40° 24'N, 117° 30'E), Xinglong
206 County, Hebei Province, China. The site is surrounded by mountains, sparsely populated, with little
207 human activities. The LUCCN ground base nodes have been installed very close to the Picarro G2301
208 tube inlet on the rooftop measurement platform building. All sensors are close to each other to ensure
209 that the measurement targets are similar, as shown in Figure 1(a).

210 We collected the measurement from 27 October 2021 to 31 July 2022, with two LUCCN sensors
211 measuring CO₂ mole fractions, temperature, pressure, relative humidity, wind direction and wind speed
212 at the sampling frequency of 1 Hz. While the reference Picarro G2301 simultaneously measured CO₂
213 dry mole fractions at the sampling frequency of 0.2 Hz.

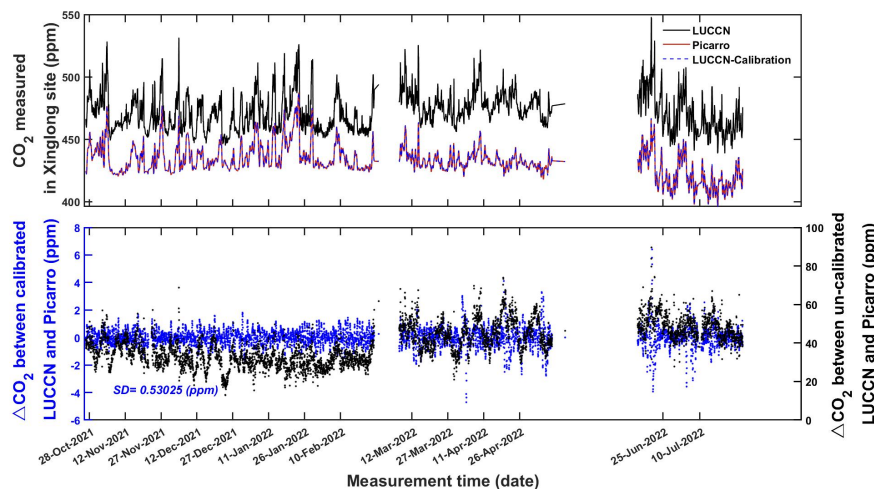
214 **3.2 Data processing and calibration**

215 Different from the laboratory observation, the responses of LUCCN sensors are affected by the
216 complex variables in the outdoor ground-based observatories. Therefore, before corrections, controlling
217 data quality is paramount for LUCCN's accuracy. Firstly, we excluded the apparent abnormal values of
218 all observed factors. Secondly, the data points larger than three times standard deviations were also
219 eliminated. Thirdly, it is necessary to select the synchronous observation data of LUCCN and Picarro
220 due to minor missing records of Picarro. After calculating the CO₂ dry molar fractions of LUCCN, we
221 interpolated the data of LUCCN and Picarro to the same sampling frequency (1 Hz).

222 With these data processing steps, we obtained the CO₂ dry mole fractions of one LUCCN node
223 (blue line) and Picarro (red line) in Figure 4, and the corresponding temperature, pressure, wind speed,
224 wind direction and relative humidity (RH) in Figure 5. There are measurements across all seasons with
225 missing observations in May. Thus, we can observe obvious seasonal variations CO₂ dry mole fractions,
226 temperature, pressure and RH. For example, CO₂ dry mole fractions are lower in summer and higher in



227 winter. It should be noted that these data were averaged over 1 hour.



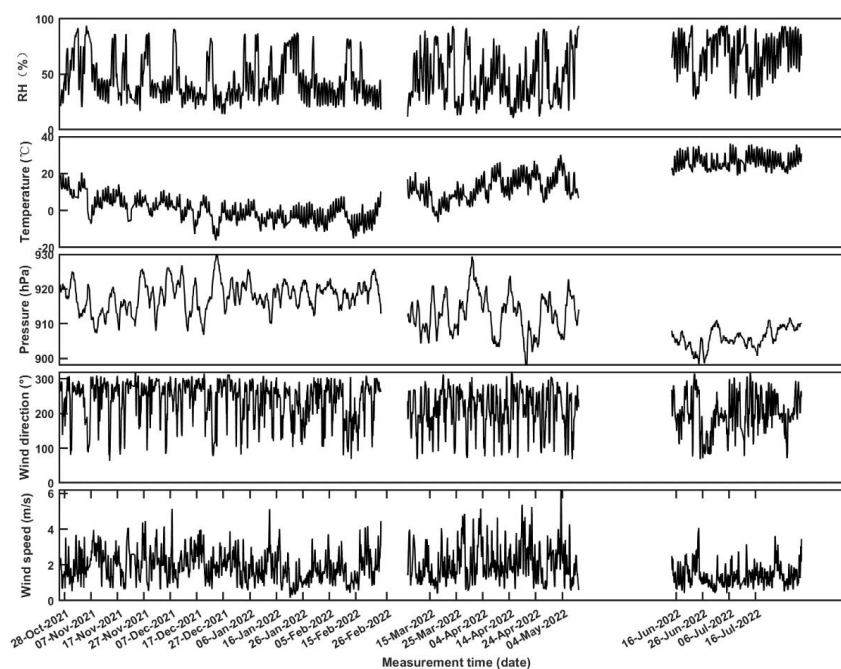
228 **Fig. 4.** (a) Time series of CO₂ dry mole fractions measured by LUCCN (black line) and Picarro (red line) at
229 Xinglong site from 27 October 2021 to 31 July 2022. And the blue dotted line presents the calibrated CO₂ mole
230 fractions of LUCCN. These data are averaged to 1 hour. (b) The black points present the differences between the
231 raw of un-calibrated LUCCN and Picarro. And the blue points present the differences between the calibrated
232 LUCCN and Picarro.

233 Based on the time series of LUCCN and Picarro CO₂ dry mole fractions in Figure 4(a), the
234 differences (ΔCO_2) of these time series (black points) are not constant with time, as shown in Figure
235 4(b). The range of ΔCO_2 is from 4 ppm to 92 ppm. While ΔCO_2 are lower in winter, and higher in
236 spring and highest in summer. Therefore, the responses of the LUCCN sensor can be related to the
237 factors such as atmospheric temperature or pressure.

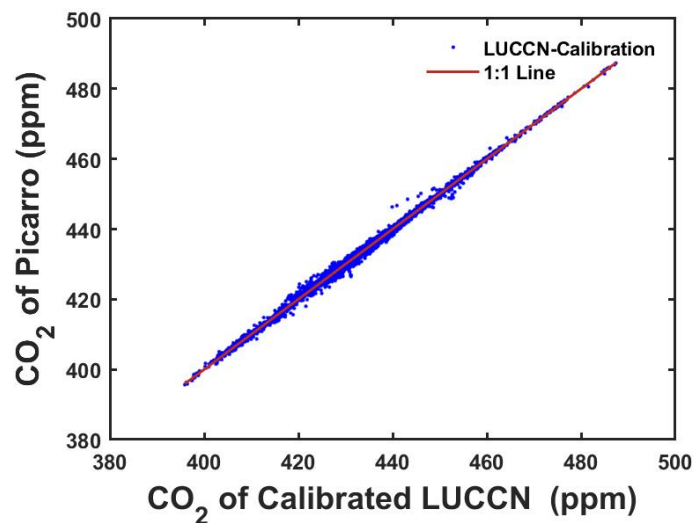
238 The last step of data processing is to reduce the influence of atmosphere on the LUCCN responses.
239 The CO₂ dry mole fractions of LUCCN were calibrated with the bias-correction method in Section 2.2.
240 With the calibration, CO₂ dry mole fractions of the corrected LUCCN data (blue dotted line) and
241 Picarro data (red line) are shown in Figure 4(a). The results show that the calibration of LUCCN is
242 highly consistent with the measurement of Picarro, and the ratios of these two sensors are close to the
243 line $CO_{2,LUCCN} = CO_{2,Picarro}$ (eg. the line 1:1) in Figure 6. Moreover, the differences between the CO₂
244 dry mole fractions of LUCCN and the raw data of Picarro in Xinglong (blue points) site are
245 significantly reduced (Figure 4(b)). The mean ΔCO_2 decreased from 39.46 ppm to 0.048 ppm at 1
246 hour and the SD decreases to 0.53 ppm at 1 hour. It should be noted that the SD of the LUCCN in



247 Xinglong site is smaller than that of the laboratory calibration results in Figure 3(b), but this is because
248 the Xinglong data used for calibration and calculation have been processed as 1-hour average data,
249 while the data during laboratory test are averaged per second. The results indicate that the calibrated
250 outdoor observation data of the LUCCN sensor can still meet the requirements of medium precision,
251 i.e., ± 1 ppm (1 SD) at 1 hour (Arzoumanian et al. 2019). In addition, SD are 0.33 ppm in autumn and
252 0.39 in winter, 0.65 ppm in spring, and 0.67 ppm in summer. During nearly a year of observation, the
253 drift of LUCCN is relatively low. Based on the above analysis, we believe that LUCCN is the effective
254 medium precision and low cost atmospheric CO₂ ground-based sensor.



255 **Fig. 5.** Time series of observations on (a) RH, (b) temperature, (c) pressure, (d) wind direction and (e) wind speed.
256 These meteorological factors were collected with CO₂ mole fractions of LUCCN (see the black line in Figure 4(a))
257 simultaneously. And these raw data are averaged to 1 hour too.



258 **Fig. 6.** The direct comparison of Picarro data and the calibrated LUCCN data at Xinglong site. The blue points are
259 the CO₂ mole fractions with calibration of LUCCN, and the red line indicates the 1:1 line.

260 **4 Cases study in pollution events**

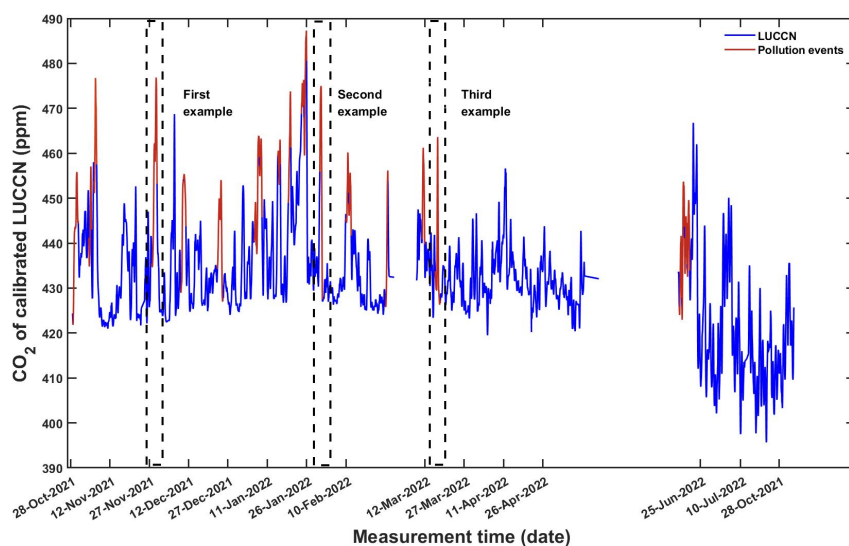
261 In order to further verify the effectiveness of the LUCCN sensor, the responses of LUCCN in
262 pollution events were compared with the observations of the Moderate Resolution Imaging
263 Spectroradiometer satellite (MODIS). During the measurement period of LUCCN, there were 27
264 pollution events in the results of MODIS. There were a few extra days when CO₂ concentrations were
265 high while unfortunately satellite data were unavailable due to cloud coverage.

266 The days of these events were selected and shown in Figure 7 with red lines. During these
267 pollution events, CO₂ dry mole fractions of these days are also higher. Such observation agreements
268 prove that LUCCN is cable of capturing upward CO₂ concentration trends during pollution events. As
269 for whether LUCCN can capture the pollution process, we selected three pollution cases to verify it.
270 Figure 8 (a), (b), (c) represent the pollution process corresponding to the dashed black boxes of Figure
271 7. The first pollution example shows that LUCCN observed a sub-peak and a peak of CO₂
272 concentrations. MODIS results show that the sub-peak corresponds to the polluted weather, and the
273 highest peak is more polluted. Before and after the peaks, the CO₂ levels observed by LUCCN were
274 relatively lower, and the corresponding images of MODIS presented cleaner weathers, except for

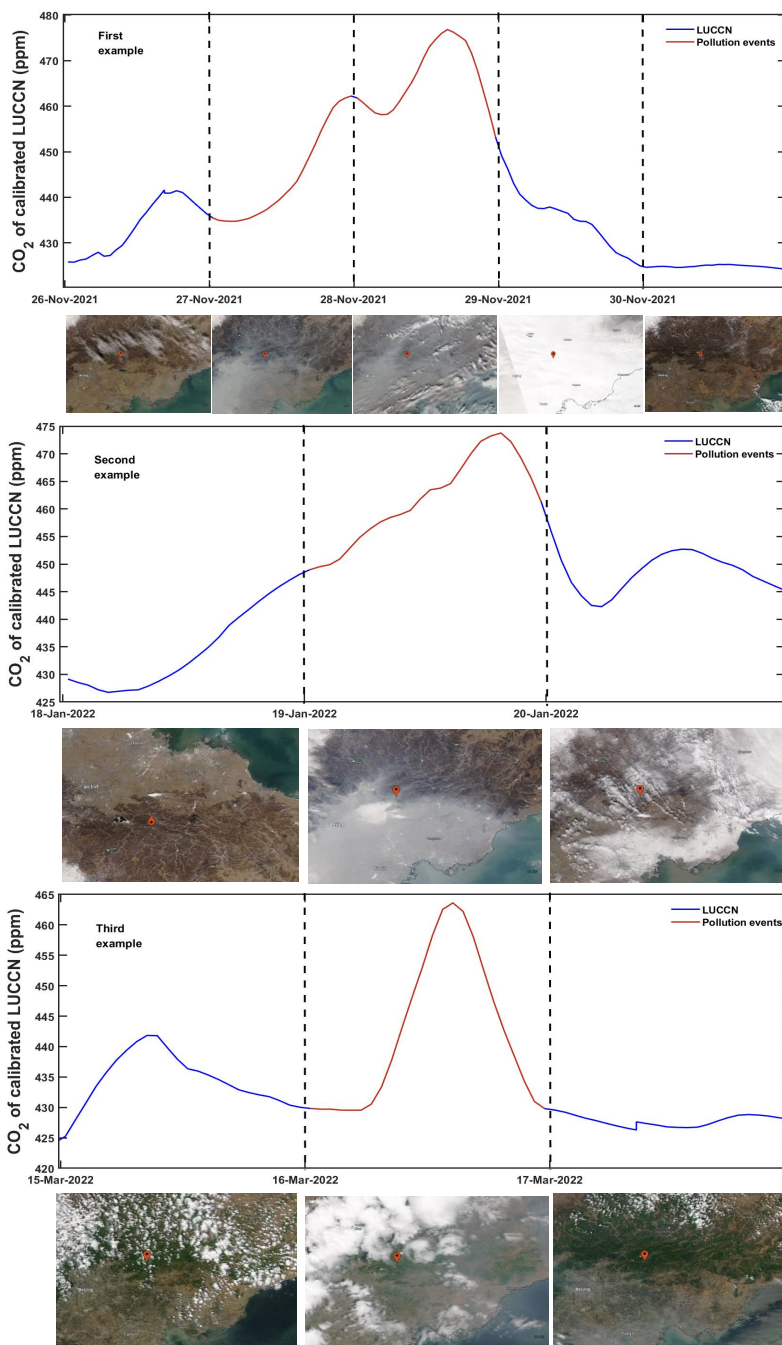


275 November 29, 2021, when the image is obscured by clouds. The second and third examples show that
276 the higher CO₂ concentrations observed by LUCCN corresponded to the pollution weather shown by
277 MODIS. Moreover, when pollution levels were low before and after polluted events, the CO₂ dry mole
278 fractions observed by LUCCN also decreased accordingly. This indicates that LUCCN is sensitive to
279 pollution events and can capture the pollution processes effectively. Comparative analysis shows that
280 the observation results of LUCCN and MODIS are in good agreement.

281 LUCCN sensors not only need to have the ability to identify pollution processes, they also need to
282 have high sensitivity to pollution events. In view of this, we would compare the differences between
283 LUCCN and Picarro in pollution events and non-pollution events respectively. The results show that in
284 the pollution events, the SD of the differences between LUCCN and Picarro is 0.367 ppm. In the 27
285 non-pollution events randomly selected, the SD of the difference is 0.363 ppm. The results indicate that
286 LUCCN has high sensitivity in both pollution and non-pollution events. Therefore, the LUCCN sensors
287 are effective to measure the changes of CO₂ mole fractions.



288 **Fig. 7.** The relationships between CO₂ mole fractions of LUCCN (blue lines) and the corresponding pollution
289 events observed by the MODIS satellite (red lines) at Xinglong site. The black dashed boxes represent three
290 examples of pollution events displayed by MODIS, which would display the measurements of LUCCN and
291 corresponding satellite images in the following figure.



292 **Fig. 8.** (a) The first example of the pollution events in Fig.7. (b) The second example of the pollution events in
293 Fig.7. (c) The third example of the pollution events in Fig. 7. The above figures are the enlarged images of the
294 dashed boxes in Fig. 7, with the black dashed line indicating the boundary of each day. The below figures are the
295 corresponding MODIS images of each day, and the red marks indicate the location of the Xinglong site.



296 5 Conclusion and outlooks

297 Low-cost urban CO₂ observation networks play a crucial role in monitoring urban CO₂ emissions
298 and estimating their impacts on the environment. In this paper, we have described the composition,
299 principle, calibration, and ground-based observations of the Low-cost UAV Coordinated Carbon
300 Observation Network - LUCCN. At present, LUCCN nodes are capable of observing CO₂
301 concentration, temperature, pressure, RH, wind direction, and wind speed, and have a comprehensive
302 design for data transmission, power supply, and equipment enclosure. Moreover, the accuracies of
303 LUCCN have been verified through calibration experiments in the laboratory and outdoor ground
304 observation. Because the relationships between the CO₂ measurements of LUCCN sensors and their
305 impact factors are not completely linear, the multi-variable non-linear regression method has been
306 adopted to calibrate the measurement data of seven LUCCN sensors in the laboratory. The calibrated
307 results show that the differences between the measurements of LUCCN and Picarro have been
308 significantly reduced. The SD of seven LUCCN sensors are all less than 1 ppm, where the maximum
309 and minimum values are 0.782 ppm and 0.594 ppm respectively with 1 second averaging window size.
310 The results show that the accuracy of the calibrated LUCCN data is higher than the medium precision
311 requirement, i.e., ± 1 ppm at 1 hour (Arzoumanian et al., 2019). This result preliminarily proves that
312 the LUCCN can measure CO₂ concentrations effectively.

313 In addition to the calibration experiments in the laboratory, we completed long-term and
314 continuous observation of LUCCN at the Xinglong Atmospheric Background Observatory from the
315 27th of October, 2021 to 31st of July, 2022. With the quality controlling and calibration, the 1 hour
316 average difference values of LUCCN and Picarro decrease from 39.46 ppm to 0.048 ppm. CO₂ dry
317 mole fractions of LUCCN and Picarro are close to 1:1. And the SD is reduced from 9.06 ppm to 0.53
318 ppm which is less than 1 ppm at 1 hour. That is, the accuracy of LUCCN still has reached the
319 requirement of medium precision. Moreover, over the one-year observation period, the drift of LUCCN
320 is small enough to be ignored. These above results further confirm that LUCCN is useful to measure
321 the surface CO₂ concentrations.

322 Not only the accuracy of LUCCN has been confirmed, but also the sensitivity to the changes of
323 CO₂ concentrations has been verified. Therefore, a comparative analysis is made with the results of the
324 satellite observation. During the observation period, there are 27 pollution events shown by MODIS



325 satellite. In the pollution events displayed by MODIS, CO₂ dry mole fractions observed by LUCCN
326 presented higher values. Moreover, LUCCN observations also showed lower CO₂ levels in clean
327 weathers before and after pollution events. These examples show that LUCCN can effectively measure
328 the changes of CO₂ concentrations. And the SD between LUCCN and Picarro in pollution events and
329 non-pollution events are 0.367 ppm and 0.363 ppm respectively. Through these analyses, LUCCN can
330 effectively observe the fluctuations of CO₂ concentrations. Not only that, the self-adaption LUCCN
331 system has been applied in the first integrated measurement campaign in Shenzhen, China. Through the
332 campaign, we found that the LUCCN system is able to increase the spatial and temporal coverage of
333 carbon emission information, especially in cases involving the detection of small, rapidly changing
334 sources and sinks (Yang et al., 2024). To sum up, the LUCCN can realize the goal of low cost and
335 medium precision CO₂ observation, it is also a powerful tool to achieve the ground CO₂ monitoring
336 network.

337 **Author contribution**

338 Xiaoyu Ren: Data curation, Methodology, Formal analysis, Writing - original draft. Dongxu Yang:
339 Conceptualization, Methodology, Supervision, Resources, Writing - review & editing. Yi Liu:
340 Investigation, Supervision, Resources. Yong Wang: Resources. Ting Wang: Data curation, Software.
341 Zhaonan Cai: Investigation, Supervision. Lu Yao: Methodology, Formal analysis. Tonghui Zhao:
342 Writing - review & editing. Jing Wang: Methodology, Formal analysis. Zhe Jiang: Conceptualization.

343 **Data availability**

344 The data are accessible by contacting the authors (renxiaoyu@mail.iap.ac.cn and
345 yangdx@mail.iap.ac.cn).

346 **Acknowledgments**

347 This work was supported by the Chinese Academy of Sciences Project for Young Scientists in
348 Basic Research (YSBR-037), the International Partnership Program of the Chinese Academy of
349 Sciences (060GJHZ2022070MI), and the MOST-ESA Dragon-5 Programme for Monitoring
350 Greenhouse Gases from Space (ID. 59355).



351 **Competing Interest**

352 The authors declare that they have no conflict of interest.

References

- Agustí-Panareda, A., McNorton, J., Balsamo, G., et al.: Global nature run data with realistic high-resolution carbon weather for the year of the Paris Agreement. *Scientific Data*. 9(1), 160. <https://doi.org/10.1038/s41597-022-01228-2>, 2022.
- Andres, Robert, J., BODEN, Thomas, A., et al.: A new evaluation of the uncertainty associated with CDIAC estimates of fossil fuel carbon dioxide emission. *Tellus B: Chemical and Physical Meteorology*. 66(1). <https://doi.org/10.3402/tellusb.v66.23616>, 2014.
- Arzoumanian, E., Vogel, F. R., Bastos, A., et al.: Characterization of a commercial lower-cost medium-precision non-dispersive infrared sensor for atmospheric CO₂ monitoring in urban areas. *Atmospheric Measurement Techniques*, 12, 2665-2677. <https://doi.org/10.5194/amt-12-2665-2019>, 2019.
- Bao, S., Wutzler, T., Koirala, S., Cuntz, M., et al.: Environment-sensitivity functions for gross primary productivity in light use efficiency models. *Agricultural and Forest Meteorology* v. 312(9), 108708. <https://doi.org/10.1016/j.agrformet.2021.108708>, 2022.
- Bréon, F. M., Broquet, G., Puygrenier, V., et al.: An attempt at estimating Paris area CO₂ emissions from atmospheric concentration measurements. *Atmos. Chem. Phys.*. 15(4), 1707-1724. <https://doi.org/10.5194/acp-15-1707-2015>, 2015.
- Broquet, Gregoire, Ciais, et al.: What would dense atmospheric observation networks bring to the quantification of city CO₂ emissions? *Atmospheric Chemistry & Physics*. 16(12), 7743-7771. <https://doi.org/10.5194/acp-16-7743-2016>, 2016.
- Delaria, E. R., Kim, J., Fitzmaurice, H. L., et al.: The Berkeley Environmental Air-quality and CO₂ Network: field calibrations of sensor temperature dependence and assessment of network scale CO₂ accuracy. *Atmospheric Measurement Techniques*. 14(8), 5487-5500. <https://doi.org/10.5194/amt-14-5487-2021>, 2021.
- Duren, R. M., Miller, C.: Measuring the carbon emissions of megacities. *Nature*. 2(8), 560-562. <https://doi.org/10.1038/nclimate1629>, 2012.
- Irène, X.-R., Elsa, D., Vuillemin, C., et al.: Diurnal, synoptic and seasonal variability of atmospheric CO₂ in the Paris megacity area. *Atmospheric Chemistry & Physics*. 18(5), 3335-3362. <https://doi.org/10.5194/acp-18-3335-2018>, 2018.
- Kim, J., Shusterman, A. A., Lieschke, K. J., Newman, C.: et al. The BERkeley Atmospheric CO₂ Observation Network: Field Calibration and Evaluation of Low-cost Air Quality Sensors. *Atmospheric Measurement Techniques*. 11(4), 1937-1946. <https://doi.org/10.5194/amt-11-1937-2018>, 2018.
- Kort, E. A., Angevine, W. M., Duren, R., et al.: Surface observations for monitoring urban fossil fuel CO₂ emissions: Minimum site location requirements for the Los Angeles megacity. *Journal of Geophysical Research: Atmosphere*. 118(3), 1577-1584. <https://doi.org/10.1002/jgrd.50135>, 2013.



- Lee, J. K., Christen, A., Ketler, R., et al.: A mobile sensor network to map carbon dioxide emissions in urban environments. *Atmospheric Measurement Techniques*. 10(2), 645–665. <https://doi.org/10.5194/amt-10-645-2017>, 2017.
- Liu, D., Sun, W., Zeng, N., et al.: Observed decreases in on-road CO₂ concentrations in Beijing during COVID-19 restrictions. *Atmospheric Chemistry and Physics*. 21(6), 4599–4614. <https://doi.org/10.5194/acp-21-4599-2021>, 2021.
- Liu, Z., He, C., Zhou, Y., et al.: How much of the world's land has been urbanized, really? A hierarchical framework for avoiding confusion. *Landscape Ecol.* 29(5), 763–771. <https://doi.org/10.1007/s10980-014-0034-y>, 2014.
- Maksyutov, S., Eggleston, S., Woo, J. H., et al.: 2019 Refinement to the 2006 IPCC Guidelines for National Greenhouse Gas Inventories. Vol 1 Chapter 6: QUALITY ASSURANCE/QUALITY CONTROL AND VERIFICATION, 2019 Refinement to the 2006 IPCC Guidelines for National Greenhouse Gas Inventories. Vol 1, 2019.
- Müller, M., Graf, P., Meyer, J., Pentina, et al.: Integration and calibration of non-dispersive infrared (NDIR) CO₂ low-cost sensors and their operation in a sensor network covering Switzerland. *Atmospheric Measurement Techniques*. 13(7), 3815–3834. <https://doi.org/10.5194/amt-13-3815-2020>, 2020.
- Park, C., Jeong, S., Park, H., et al.: Challenges in Monitoring Atmospheric CO₂ Concentrations in Seoul Using Low-Cost Sensors. *Asia-Pacific Journal of the Atmospheric Sciences*. 57(10), 574–553. <https://doi.org/10.1007/s13143-020-00213-2>, 2020.
- Ries, L. C., Ries L.: Standardized and automated data quality assurance at GAW Stations - concept, methods and tools. in GAW Report Nr. 213, 17th WMO/IAEA Meeting on Carbon Dioxide, other Greenhouse Gases and Related Tracers Measurement Techniques. 117–129, 2013.
- Rosenzweig, C., Solecki, W., Hammer, S. A., et al.: Cities lead the way in climate–change action. *Nature*. 467, 909–911. <https://doi.org/10.1038/467909a>, 2010.
- Shusterman, A. A., Kim, J., Lieschke, K. J., et al.: Observing local CO₂ sources using low-cost, near-surface urban monitors. *Atmospheric Chemistry and Physics*. 18(18), 13773–13785. <https://doi.org/10.5194/acp-18-13773-2018>, 2018.
- Staufer, J., Broquet, G., Bréon, F.-M., et al.: The first 1-year-long estimate of the Paris region fossil fuel CO₂ emissions based on atmospheric inversion. *Atmospheric Chemistry and Physics*. 16(22), 14703–14726. <https://doi.org/10.5194/acp-16-14703-2016>, 2016.
- Teige, Virginia, E., Shusterman, Alexis, A., Newman, et al.: The Berkeley Atmospheric CO₂ Observation Network: initial evaluation. *Atmospheric Chemistry and Physics*. 16(21), 13449–13463. <https://doi.org/10.5194/acp-16-13449-2016>, 2016.
- Turnbull, J. C., Sweeney, C., Karion, A., et al.: Toward quantification and source sector identification of fossil fuel CO₂ emissions from an urban area: Results from the INFLUX experiment. *Journal of Geophysical Research: Atmosphere*. 120(1), 292–312. <https://doi.org/10.1002/2014JD022555>, 2015.
- Turner, A. J., Shusterman, A. A., Mcdonald, B. C., et al.: Network design for quantifying urban CO₂ emissions: assessing trade-offs between precision and network density. *Atmospheric Chemistry and Physics*. 16(21), 13465–13475. <https://doi.org/10.5194/acp-16-13465-2016>, 2016.
- Verhulst, K. R., Karion, A., Kim, J., et al.: Carbon dioxide and methane measurements from the Los Angeles Megacity Carbon Project - Part 1: calibration, urban enhancements, and uncertainty



- estimates. *Atmospheric Chemistry and Physics*. 17(13), 8313–8341. <https://doi.org/10.5194/acp-17-8313-2017>, 2017.
- Wu, L., Broquet, G., Ciais, P., et al.: What would dense atmospheric observation networks bring to the quantification of city CO₂ emissions? *Atmospheric Chemistry and Physics*. 16(12), 7743–7771. <https://doi.org/10.5194/acp-16-7743-2016>, 2016.
- Yang, D., Zhao, T., Yao, L., et al.: Toward establishing a low-cost uav coordinated carbon observation network(luccn): first integrated campaign in china. *Advances in Atmospheric Sciences*. 41(1), 1–7. <https://doi.org/10.1007/s00376-023-3107-5>, 2024.